SEARCH FOR THE FLAVOR-CHANGING NEUTRAL CURRENT IN TOP PAIR EVENTS WITH AN ASSOCIATED PHOTON USING 13 TEV PROTON-PROTON COLLISION DATA COLLECTED WITH THE ATLAS DETECTOR

by

JASON TYLER BARKELOO

A DISSERTATION

Presented to the Department of Physics
and the Graduate School of the University of Oregon
in partial fulfillment of the requirements
for the degree of
Doctor of Philosophy

March 2020

DISSERTATION APPROVAL PAGE

Student: Jason Tyler Barkeloo

Title: Search for the Flavor-Changing Neutral Current in Top Pair Events With an Associated Photon Using 13 TeV Proton-Proton Collision Data Collected With the ATLAS Detector

This dissertation has been accepted and approved in partial fulfillment of the requirements for the Doctor of Philosophy degree in the Department of Physics by:

David Strom	Chair
James Brau	Advisor
Spencer Chang	Core Member
Dev Sinha	Institutional Representative

and

Janet Woodruff-Borden	Vice Provost and Dean of the Graduate School

Original approval signatures are on file with the University of Oregon Graduate School.

Degree awarded March 2020

DISSERTATION ABSTRACT

Jason Tyler Barkeloo

Doctor of Philosophy

Department of Physics

March 2020

Title: Search for the Flavor-Changing Neutral Current in Top Pair Events With an Associated Photon Using 13 TeV Proton-Proton Collision Data Collected With the ATLAS Detector

Abstract for FCNC here.

This dissertation includes previously published and unpublished co-authored material.

CURRICULUM VITAE

NAME OF AUTHOR: Jason Tyler Barkeloo

GRADUATE AND UNDERGRADUATE SCHOOLS ATTENDED:
University of Oregon, Eugene, Oregon
Miami University, Oxford, Ohio
Wittenberg University, Springfield, Ohio

DEGREES AWARDED:
Doctor of Philosophy, Physics, 2020, University of Oregon
Master of Sceience, Physics, 2012, Miami University
Bachelor of Science, Physics, 2010, Wittenberg Univeristy

PROFESSIONAL EXPERIENCE:

University of Oregon, Graduate Research Assistant, ATLAS Experiment, June 2014-Present

University of Oregon, Graduate Teaching Assistant, September 2012-June 2014

Miami University, Teaching and Research Assistant, August 2010 - May 2012

Wittenberg University, Undergraduate Researcher, August 2008 - May 2010

GRANTS, AWARDS AND HONORS:

Weiser Senior Teaching Assistant Award – University of Oregon – 2014

American Association of Physics Teachers Outstanding Teaching Assistant – Miami University – 2012

PUBLICATIONS:

A. Hachtel, J. Kleykamp, D. Kane, M. Marshall, B. Worth, J. Barkeloo, J. Kangara, J. Camenisch, M. Gillette, S. Bali. "An undergraduate lab on measurement of radiative broadening in atomic vapor", Am. J. Phys. **81**(6), 471 (2013).

J. Kangara, A. Hachtel, M. C. Gillette, J. Barkeloo, E. Clements, S. Bali. "Design and construction of cost-effective fail-safe tapered amplifier systems for laser cooling and trapping experiments", Am. J. Phys. **82**(8), 805 - 817 (2014).

TABLE OF CONTENTS

Chapter Page

Chapter | Page

LIST OF FIGURES

Figure Page

Figure Page

LIST OF TABLES

Table Page

CHAPTER I

THE LARGE HADRON COLLIDER AND THE ATLAS DETECTOR

This chapter details the experimental details of the collider complex at the LHC and specifically the ATLAS detector used to produce, collect, and measure various particle properties. The subsystems of the ATLAS detector are described in detail.

1.1. The Large Hadron Collider

The LHC is the world's largest and most energetic particle accelerator. As a hadron collider the LHC collides particles made up of quarks, typically proton-proton collisions. Protons, as opposed to electrons/positrons at a previous collider such as LEP, have much higher mass and have a significantly smaller amount of energy loss during acceleration due to synchrotron radiation (which scales as $\frac{1}{m^4}$). Due to this the LHC is able to reach a much higher center of mass energy using the same circular ring used by LEP. This higher energy comes at a cost though. Due to hadrons being made up of constituent partons (quarks and gluons) not all of which interact in any given collision the particles that dont take place in the hard interaction are left over and create a 'messier' environment in the detectors. Whereas in lepton colliders all of the energy that goes into the collision is present in the final state particles coming from the interaction point. The implication of this is that hadron colliders cannot known the momentum along the beam axis and only know the momentum in the transverse plane due to conservation of momentum.

The LHC is housed in a 27 km ring running beneath the Franco-Swiss border near Geneva, Switzerland and accelerates beams of protons (ions) to a center of mass energy of 13 TeV (5 TeV) using two counterpropagating circular beams around the

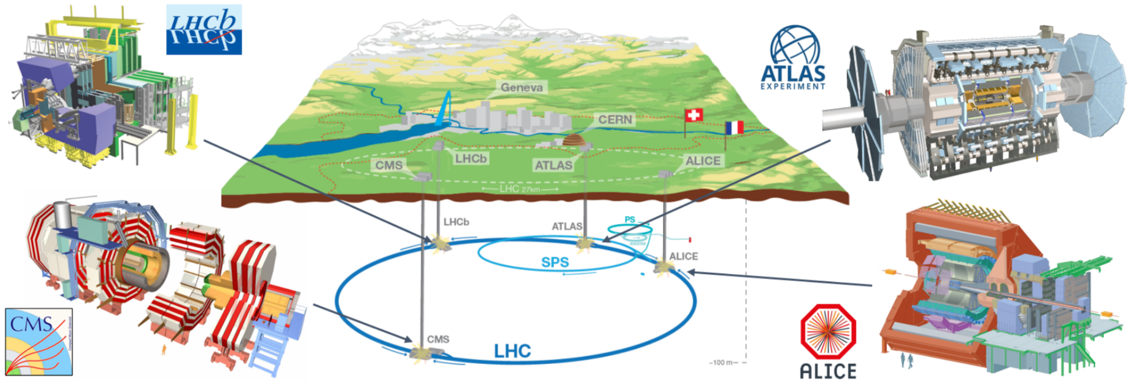

FIGURE 1.1. Map of LHC and the various detector experiments: ATLAS, CMS, LHCb, and ALICE located under the Franco-Swiss border near Geneva[35]

ring. The particles are then collided at one of the four primary interaction points, each of which house a dedicated detector as shown in Figure 3.1.

In addition to the LHC beam line the accelerator uses a series of smaller accelerators to increase the energy of the particles before being introduced into the LHC. This accelerator complex is detailed in Figure 3.2. The start of the accelerator chain, and source of LHC protons, is the Linear Accelerator 2 (LINAC 2, purple) where hydrogen gas is placed inside of an electric field which separates the protons and electrons. The remaining protons are passed through radiofrequency (RF) cavities and accelerated to 50 MeV using electric fields which oscillate at a frequency specific to the distance between any two RF cavities.

After leaving LINAC 2 the protons are injected into the Proton Synchrotron Booster (BOOSTER, light purple) and accelerated to 1.4 GeV before being passed to the Proton Synchrotron (PS, magenta) in two batches with a separation of 1.2 seconds. The PS accelerates the protons to 25 GeV to be injected into the Super Proton Synchrotron (SPS, blue) in a series of four batches seperated by 3.6 seconds and are accelerated to 450 GeV. The SPS is the second largest accelerator in the complex. After being reaching the 450 GeV of the SPS the particles are split and

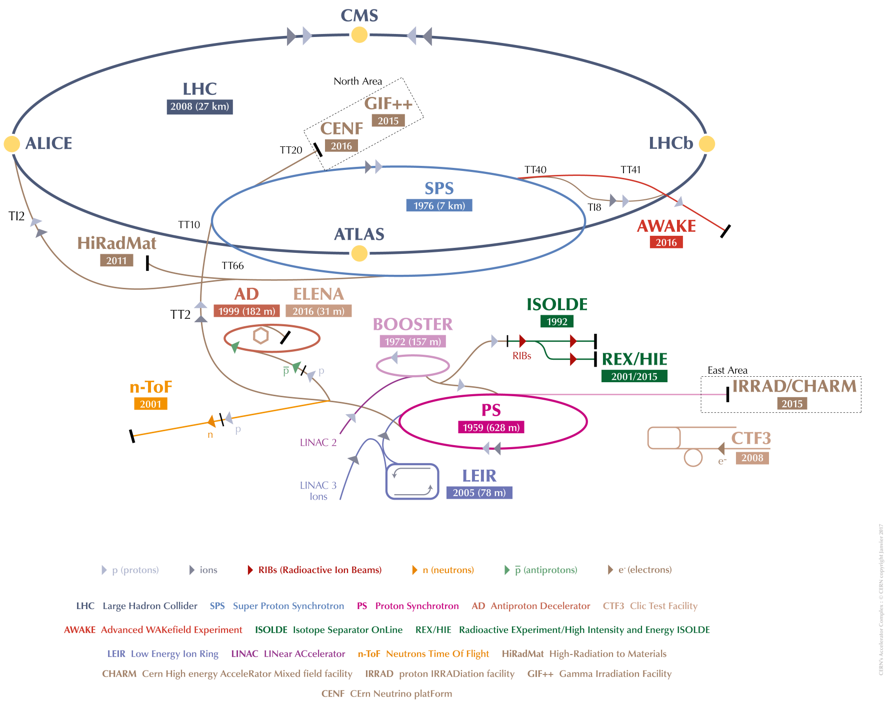

FIGURE 1.2. Schematic of the CERN accelerator complex.[32]

injected into the LHC in opposing directions where they are further accelerated to a collision energy of 6.5 TeV per beam leading to a center of mass energy of 13 TeV for the LHC during Run-2.

The first proton-proton collisions were produced in the LHC in 2008 at the injection energy of the SPS, $\sqrt{s}$ = 900 GeV. During testing a faulty electrical connection caused a magnet quench, a sudden loss of superconductivity, to occur. This broke the nearby magnets and caused a delay in operations until late 2009 when LHC Run-1 began at a collision energy of $\sqrt{s} = 7$ TeV and later raised to $\sqrt{s} = 8$ TeV in 2012 to complete Run-1. Various upgrade and repairs on the LHC occured throughout the long shutdown between 2012-2015 where the center of mass energy was increased to the LHC Run-2 energy of $\sqrt{s} = 13$ TeV.

1.1.1. LHC Magnets

The energies achieved in the collisions are only possible due to the LHC magnets that bend and focus the colliding particles. The LHC uses the most powerful magnet technology that can be produced on an industrial scale. There are 1232 superconducting dipole magnets each being 15m in length, weighing 35 tonnes, and producing uniform magnetic fields of up to 8.4 T. The niobium-titanium cables must be cooled to 1.9 K and operate with a current of 11,800 A. Of these 1232 magnets 1104 are used to bend the particles around the ring and the remaining 128 are used in the beam dump. To achieve the same center of mass energy using standard non-superconducting magnets the 27 km LHC would instead have to be upwards of 120 km long.

Since the bunches of particles are charged they will naturally diverge while traveling if not focused. To correct for this an additional 392 quadrupole magnets, 5-7m in length, are used to focus the beam. These quadrupoles are used in pairs: one which focuses in the horizontal plane and defocuses in the vertical plane and the other focuses in the vertical plane and defocuses in the horizontal plane. Together these magnets can keep the beam squeezed to a usable size. All of these magnets have two aperatures, one for each of the counter-propagating beams.

1.1.2. Luminosity

The amount of data collected at collider experiments is determined not only by the center of mass energy of colliding particles but also the rate of events produced. This rate is called the luminosity and can be determined by the square of the number of particles in each bunch (since any one in one bunch can interact with any one in the other), the time between bunches, and the cross section of the bunch (or probability of a collision).

$$\mathcal{L} = \frac{1}{\sigma}\frac{dN}{dt}$$

For any given proton-proton pair the luminosity can be expressed as:

$$\mathcal{L} = \frac{1}{4\pi\sigma_x\sigma_y}$$

and can be expanded for the whole beam with the inclusion of the number of protons per bunch (N_1 and N_2), the number of bunches (N_b), and the frequency at which the bunches overlap (f) to:

$$\mathcal{L} = \frac{N_1 N_2 N_b f}{4\pi\sigma_x\sigma_y}$$

which can be iterated over the running time of the LHC (the total time with beams of proper size and energy propagating through the LHC) giving the total delivered luminosity. This total integrated luminosity as a function of time during LHC Run-2 is shown in Figure 3.3. This luminosity value can be mulitplied by the probability, or cross section, of any particular final state to obtain the number of times that final state is produced with a given luminosity.

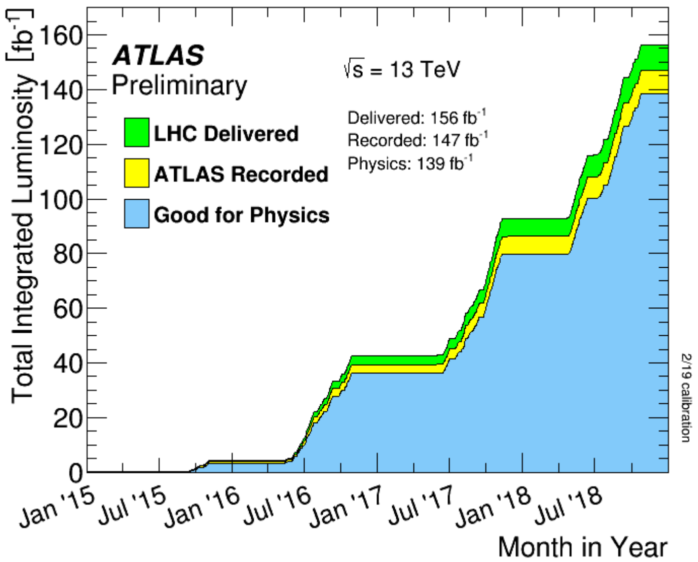

FIGURE 1.3. Total integrated luminosity as a function of time delivered by the LHC(green), recorded (yellow) and declared good for physics analysis (blue) by the ATLAS detector throughout Run 2 consisting entirely of 13 TeV *pp* collisions (figure from the ATLAS Collaboration).

1.1.3. Pileup

Increasing the luminosity is very beneficial for increasing the statistics needed when searching for rare events but it brings additional challenges as well. Most interactions at any given detector are not hard-scatter events that correspond to poentially interesting physics cases but are instead soft collisions which create noise in the various detector experiments. The LHC works hard to deliver as much data to the experiments as possible and delivers bunches of protons at a time. It is possible for multiple pairs of protons to undergo these soft ineleastic collisions at a time. The average number of interactions per bunch crossing, or pileup $\langle \mu \rangle$, for Run-2 was 33.7, shown in Figure 3.4. The pileup must be accounted for when separating the tracks and energy deposited within a detector from an interesting hard-scatter event from the other soft collisions which occur at nearly the same time. The difficulty of

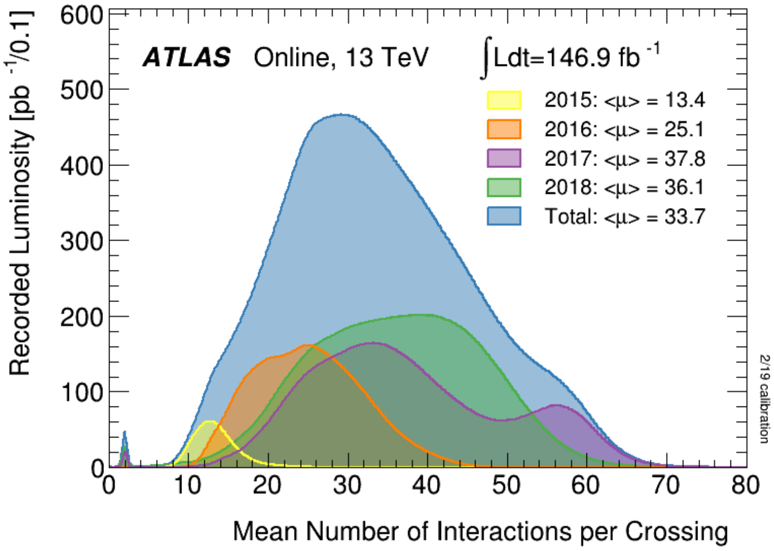

FIGURE 1.4. Luminosity-weighted distribution of the mean number of interactions per bunch crossing for the entirety of Run 2 shown by individual years, 2015 (yellow), 2016(orange), 2017 (purple), 2018 (green), as well as an integrated total (blue) (figure from the ATLAS Collaboration).

separating out one event from another can be seen in Figure 3.5 where there are 28 reconstructed verticies. An extreme case of 65 reconstructed verticies is also shown in Figure 3.6. As the LHC will continue to operate in the future at higher and higher luminosities the amount of pileup that will need to be dealt with will continue to increase.

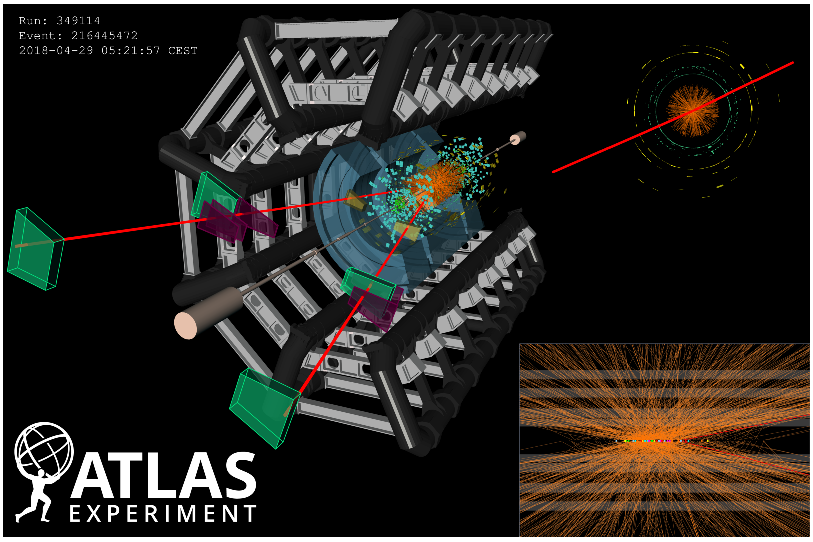

FIGURE 1.5. A candidate dimuon event ($Z \to \mu^+\mu^-$) with 28 reconstructed verticies collected in 2018 with the ATLAS detector.

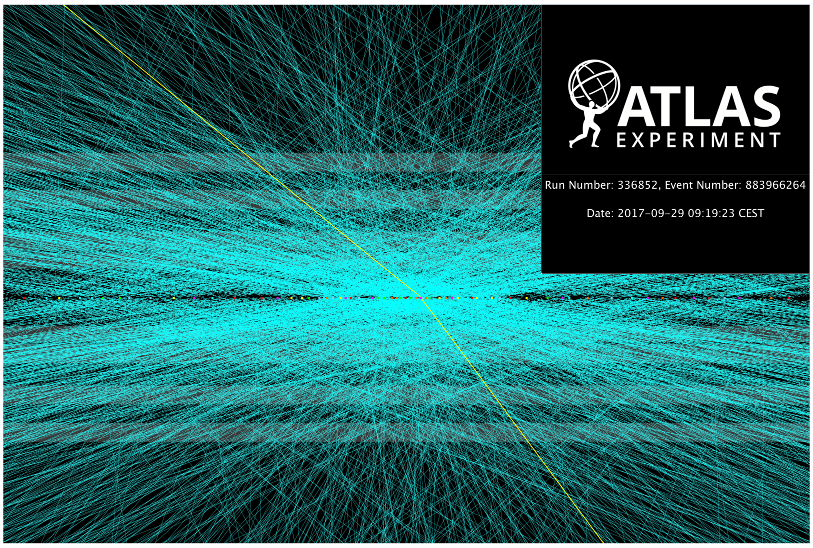

FIGURE 1.6. A candidate dimuon event ($Z \to \mu^+\mu^-$) with 65 reconstructed verticies collected in 2017 with the ATLAS detector.

1.2. The ATLAS Detector

Section:ATLAS

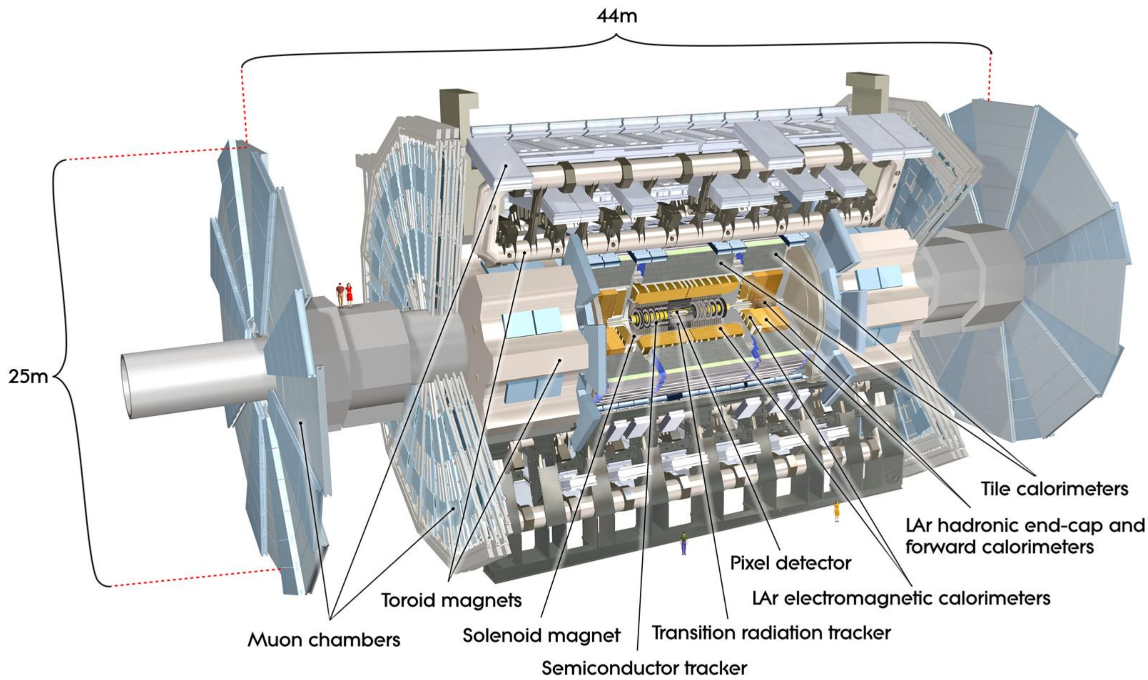

FIGURE 1.7. Schematic of the ATLAS detector.[33]

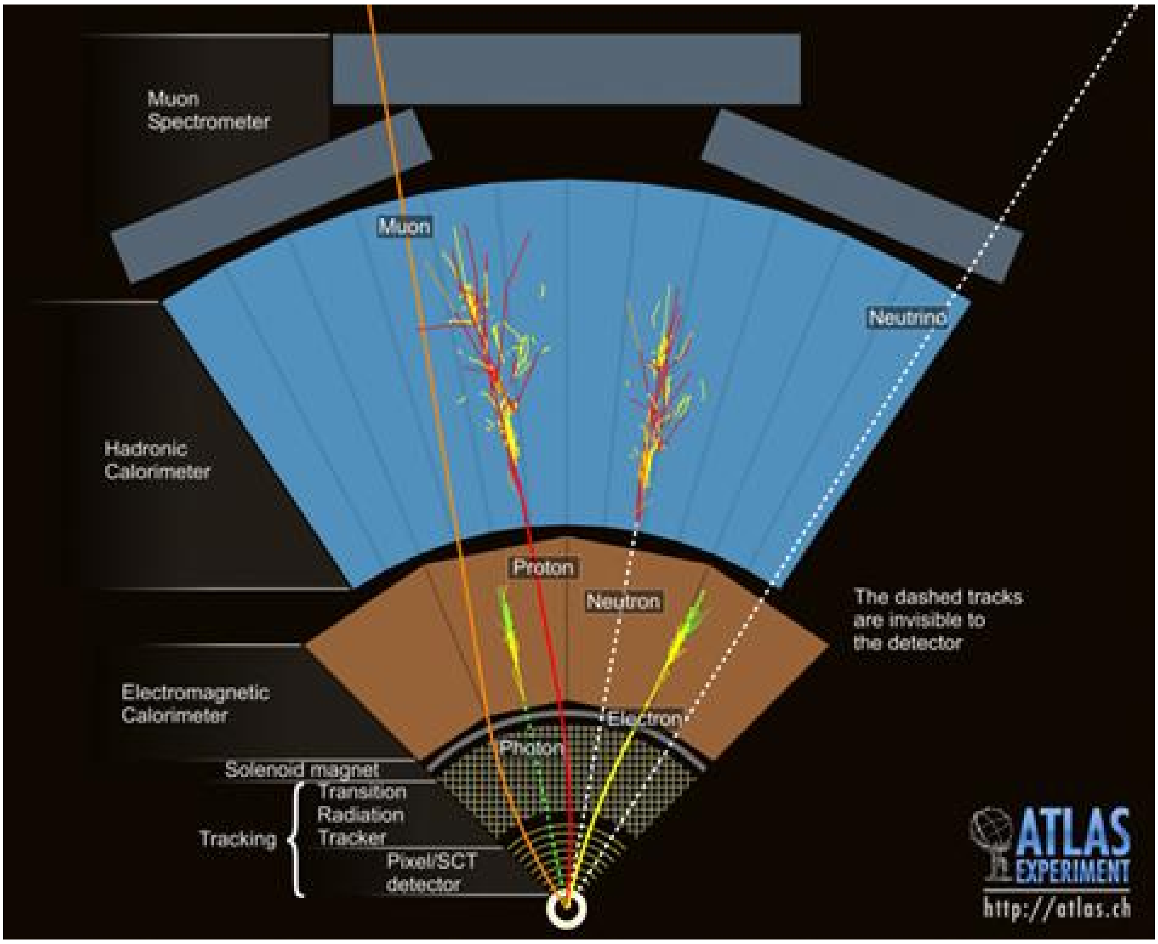

FIGURE 1.8. Cross section of a simulated ATLAS detector showing how various particles interact with ATLAS subsystems.[34]

1.2.1. Coordinate System

Coords

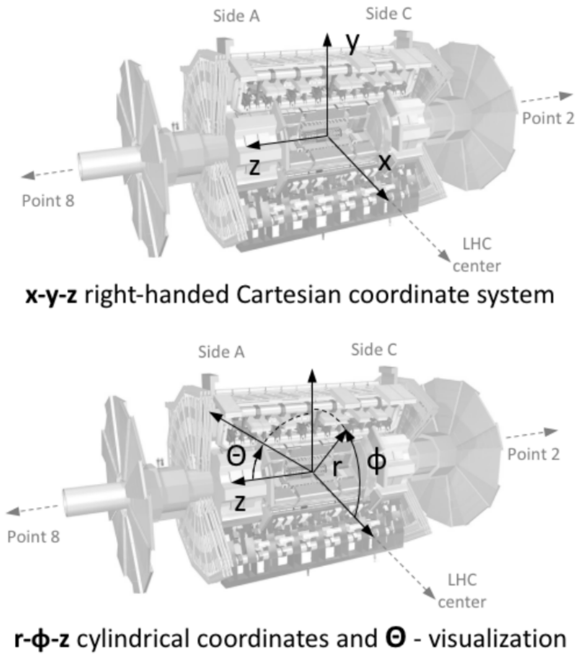

FIGURE 1.9. Coordinate system used in the ATLAS Collaboration.[35]

1.2.2. Magnet Setup

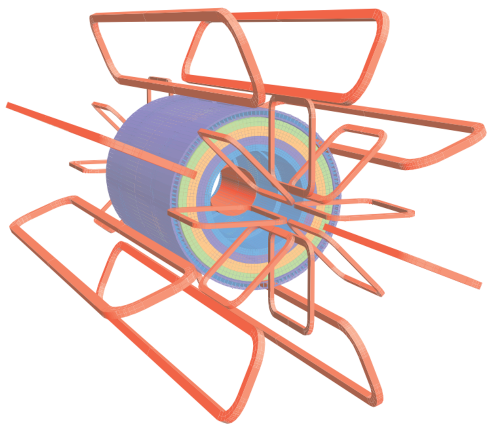

FIGURE 1.10. Schematic of the windings of the ATLAS magnet.[33]

1.2.3. Inner Detector

Inner

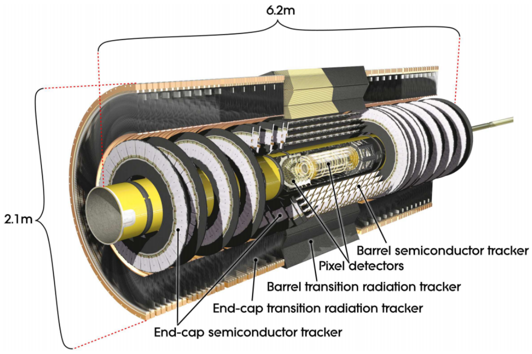

FIGURE 1.11. Schematic of the ATLAS inner detector.[33]

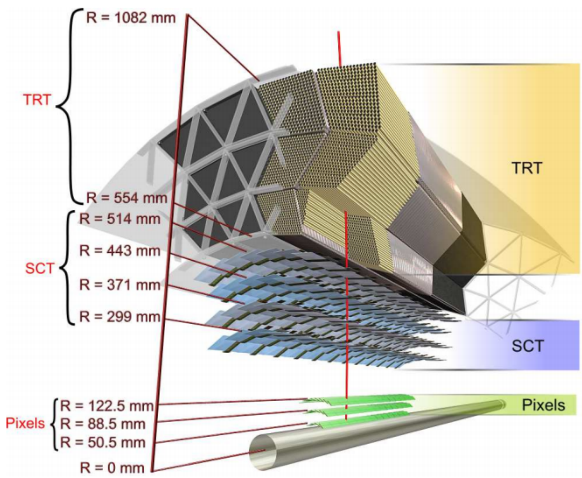

FIGURE 1.12. Blown up schematic of the ATLAS inner detector with more detail.[33]

1.2.4. Middle Layers, EMCal, HCal

Middle chunks

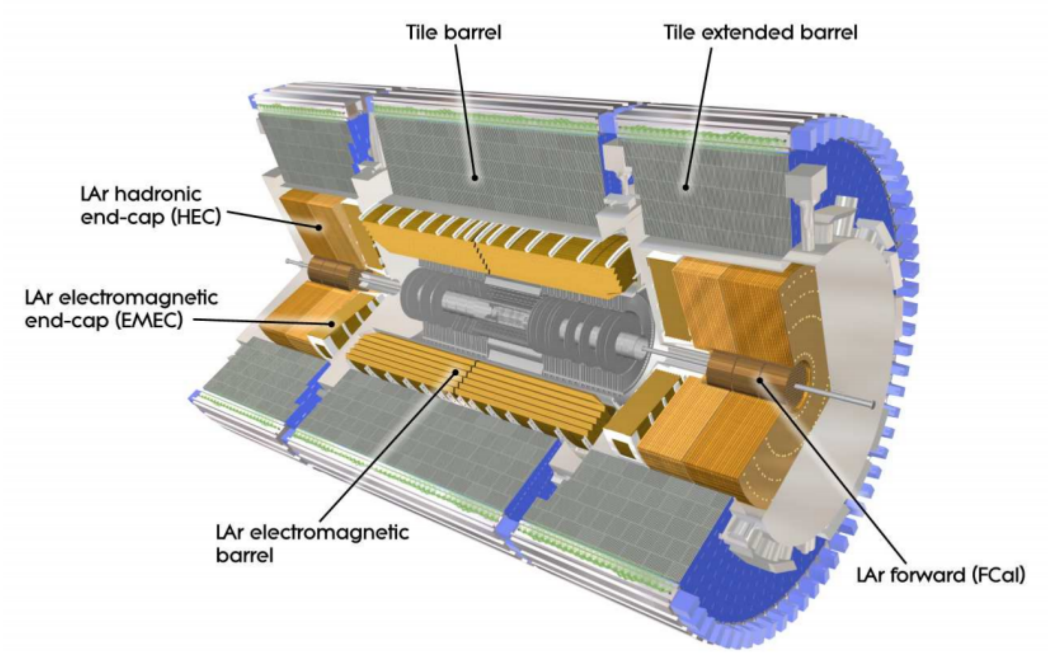

FIGURE 1.13. Schematic of the ATLAS hadronic and electromagnetic calorimeter systems.[33]

1.2.5. Muon Calorimeter

Muons have to get picked up I guess

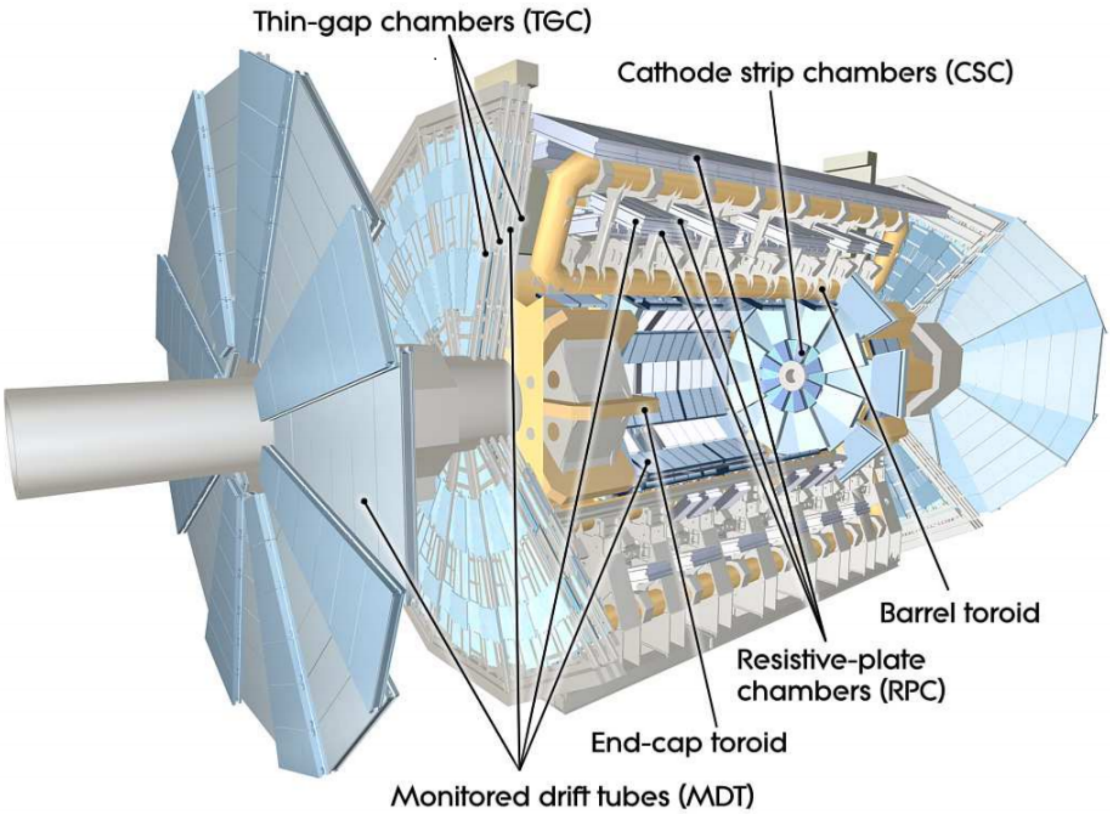

FIGURE 1.14. Schematic of the ATLAS muon detector.[33]

1.2.6. Trigger and Data Acquisition

All of these subsystems lead into actual data farm

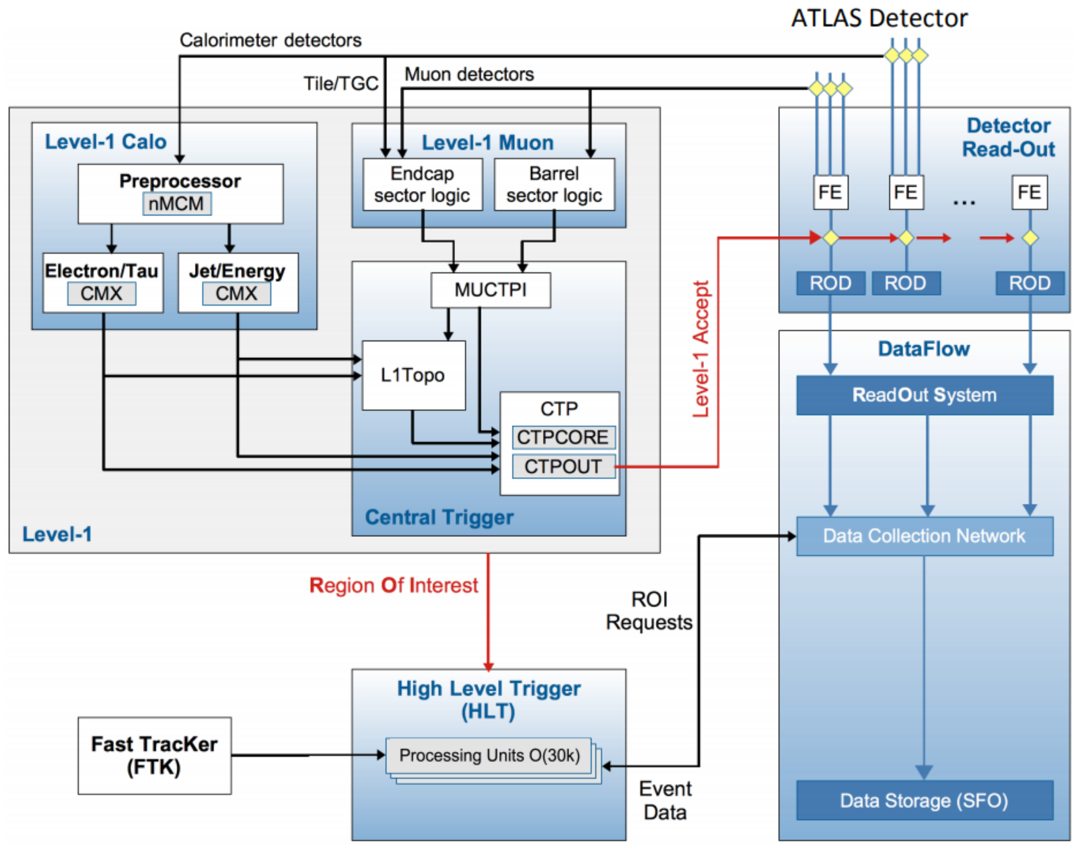

FIGURE 1.15. Flow diagram of the ATLAS trigger and data acquisition system used in Run 2.[36]

1.2.6.1. L1Calo

1.2.6.2. HLT

CHAPTER II

SIMULATION

2.1. Simulation of pp collisions

2.1.1. MC Generators Used for LHC Physics

2.1.2. Detector Simulation

2.1.3. Showering in the Detector

2.2. Object Reconstruction

2.2.1. Electrons

2.2.2. Photons

2.2.3. Jets

2.2.3.1. B-Jets

2.2.4. Muons

2.2.5. Creation of FCNC Signal Events

2.2.5.1. MadGraph5 amc@NLO

Comparison of kinematics between standard ttbar events ATLAS Production of these events TopQ1 Slimming/Skimming

CHAPTER III

SEARCH STRATEGY

3.1. Major Backgrounds

3.2. Event Reconstruction

3.3. Data and Simulation Event PreSelection

3.4. Control and Validation Regions

3.5. Signal Region

3.6. Neural Network

3.6.1. Architecture and Studies

CHAPTER IV

RESULTS

4.1. Uncertainties

4.2. Statistical Treatment of Results

4.3. Limit on Branching Ratio t$\rightarrow$qγ

CHAPTER V

COMPLEMENTARY SEARCHES AND OUTLOOK

5.1. Comparison with Complementary Searches

5.2. Future Directions

HL-LHC and Beyond Future prospectives at Linear Colliders? - https://www.sciencedirect.com/

5.3. Conclusion

REFERENCES CITED

[1] S. L. Glashow. Partial Symmetries of Weak Interactions. *Nucl. Phys.*, 22:579–588, 1961.

[2] Peter W. Higgs. Broken Symmetries and the Masses of Gauge Bosons. *Phys. Rev. Lett.*, 13:508–509, 1964. [,160(1964)].

[3] F. Englert and R. Brout. Broken Symmetry and the Mass of Gauge Vector Mesons. *Phys. Rev. Lett.*, 13:321–323, 1964. [,157(1964)].

[4] Steven Weinberg. A Model of Leptons. *Phys. Rev. Lett.*, 19:1264–1266, 1967.

[5] Abdus Salam. Weak and Electromagnetic Interactions. *Conf. Proc.*, C680519:367–377, 1968.

[6] Georges Aad et al. Observation of a new particle in the search for the Standard Model Higgs boson with the ATLAS detector at the LHC. *Phys. Lett.*, B716:1–29, 2012.

[7] Serguei Chatrchyan et al. Observation of a new boson at a mass of 125 GeV with the CMS experiment at the LHC. *Phys. Lett.*, B716:30–61, 2012.

[8] F. Abe et al. Observation of top quark production in $\bar{p}p$ collisions. *Phys. Rev. Lett.*, 74:2626–2631, 1995.

[9] The ATLAS collaboration. Measurement of the top quark mass in the $t\bar{t} \rightarrow$ lepton+jets channel from $\sqrt{s}$=8 TeV ATLAS data. 2017.

[10] M. Tanabashi et al. Review of Particle Physics. *Phys. Rev.*, D98(3):030001, 2018.

[11] J. J. Cao, G. Eilam, M. Frank, K. Hikasa, G. L. Liu, I. Turan, and J. M. Yang. SUSY-induced FCNC top-quark processes at the large hadron collider. *Phys. Rev.*, D75:075021, 2007.

[12] Junjie Cao, Zhaoxia Heng, Lei Wu, and Jin Min Yang. R-parity violating effects in top quark FCNC productions at LHC. *Phys. Rev.*, D79:054003, 2009.

[13] G. Eilam, J. L. Hewett, and A. Soni. Rare decays of the top quark in the standard and two Higgs doublet models. *Phys. Rev.*, D44:1473–1484, 1991. [Erratum: Phys. Rev.D59,039901(1999)].

[14] Yuval Grossman. Introduction to flavor physics. In *Flavianet School on Flavour Physics Karlsruhe, Germany, September 7-18, 2009*, pages 111–144, 2014. [,73(2014)].

[15] Nicola Cabibbo. Unitary Symmetry and Leptonic Decays. *Phys. Rev. Lett.*, 10:531–533, 1963. [,648(1963)].

[16] Makoto Kobayashi and Toshihide Maskawa. CP Violation in the Renormalizable Theory of Weak Interaction. *Prog. Theor. Phys.*, 49:652–657, 1973.

[17] Lincoln Wolfenstein. Parametrization of the Kobayashi-Maskawa Matrix. *Phys. Rev. Lett.*, 51:1945, 1983.

[18] S. L. Glashow, J. Iliopoulos, and L. Maiani. Weak Interactions with Lepton-Hadron Symmetry. *Phys. Rev.*, D2:1285–1292, 1970.

[19] S. W. Herb et al. Observation of a Dimuon Resonance at 9.5-GeV in 400-GeV Proton-Nucleus Collisions. *Phys. Rev. Lett.*, 39:252–255, 1977.

[20] S. Abachi et al. Search for high mass top quark production in $p\bar{p}$ collisions at $\sqrt{s} = 1.8$ TeV. *Phys. Rev. Lett.*, 74:2422–2426, 1995.

[21] Markus Cristinziani and Martijn Mulders. Top-quark physics at the Large Hadron Collider. *J. Phys.*, G44(6):063001, 2017.

[22] J. A. Aguilar-Saavedra. Top flavor-changing neutral interactions: Theoretical expectations and experimental detection. *Acta Phys. Polon.*, B35:2695–2710, 2004.

[23] David Atwood, Laura Reina, and Amarjit Soni. Phenomenology of two Higgs doublet models with flavor changing neutral currents. *Phys. Rev.*, D55:3156–3176, 1997.

[24] J. A. Aguilar-Saavedra and B. M. Nobre. Rare top decays t —¿ c gamma, t —¿ cg and CKM unitarity. *Phys. Lett.*, B553:251–260, 2003.

[25] J. A. Aguilar-Saavedra. Effects of mixing with quark singlets. *Phys. Rev.*, D67:035003, 2003. [Erratum: Phys. Rev.D69,099901(2004)].

[26] Jin Min Yang, Bing-Lin Young, and X. Zhang. Flavor changing top quark decays in r parity violating SUSY. *Phys. Rev.*, D58:055001, 1998.

[27] Kaustubh Agashe, Gilad Perez, and Amarjit Soni. Collider Signals of Top Quark Flavor Violation from a Warped Extra Dimension. *Phys. Rev.*, D75:015002, 2007.

[28] Mark Trodden. Electroweak baryogenesis. *Rev. Mod. Phys.*, 71:1463–1500, 1999.

[29] G. C. Branco, P. M. Ferreira, L. Lavoura, M. N. Rebelo, Marc Sher, and Joao P. Silva. Theory and phenomenology of two-Higgs-doublet models. *Phys. Rept.*, 516:1–102, 2012.

[30] Andreas Crivellin and Ulrich Nierste. Chirally enhanced corrections to FCNC processes in the generic MSSM. *Phys. Rev.*, D81:095007, 2010.

[31] Georges Aad et al. Search for flavour-changing neutral currents in processes with one top quark and a photon using 81 fb^{-1} of pp collisions at $\sqrt{s} = 13$ TeV with the ATLAS experiment. 2019.

[32] Esma Mobs. The CERN accelerator complex. Complexe des accélérateurs du CERN. Jul 2016. General Photo.

[33] The ATLAS Experiment at the CERN Large Hadron Collider. *J. Instrum.*, 3:S08003. 437 p, 2008.

[34] Joao Pequenao. Event Cross Section in a computer generated image of the ATLAS detector. Mar 2008.

[35] Fabian Kuger. Signal formation processes in micromegas detectors and quality control for large size detector construction for the atlas new small wheel. 08 2017.

[36] Moritz Backes. The ATLAS Trigger System: Ready for Run-2. *PoS*, LeptonPhoton2015:045, 2016.